Title

Electrotaxis of cardiac progenitor cells, cardiac fibroblasts, and induced pluripotent stem cell-derived cardiac progenitor cells requires serum and is directed via PI3′K pathways

Journal

Heart Rhythm, 14(11)

ISSN

1547-5271

Authors

Frederich, Bert J
Timofeyev, Valeriy
Thai, Phung N
et al.

Publication Date

2017-11-01

DOI

10.1016/j.hrthm.2017.06.038

Peer reviewed

HHS Public Access

Author manuscript

Heart Rhythm. Author manuscript; available in PMC 2018 November 01.

Published in final edited form as:

Heart Rhythm. 2017 November ; 14(11): 1685–1692. doi:10.1016/j.hrthm.2017.06.038.

Electrotaxis of Cardiac Progenitor Cells, Cardiac Fibroblasts, and Induced Pluripotent Stem cell-derived Cardiac Progenitor Cells requires serum and is directed *via* PI3′K pathways

Bert J Frederich, Ph.D.[1], **Valeriy Timofeyev, Ph.D.**[1], **Phung N Thai, Ph.D.**[1], **Michael J. Haddad**[1], **Adam Poe, Ph.D.**[1], **Victor C Lau, B.S.**[1], **Maryam Moshref, M.S.**[1], **Anne A. Knowlton, M.D.**[1,2], **Padmini Sirish, Ph.D.**[1], and **Nipavan Chiamvimonvat, M.D.**[1,2]

[1]Division of Cardiovascular Medicine, University of California, Davis, CA

[2]Department of Veterans Affairs, Northern California Health Care System, Mather, CA

Abstract

Background—The limited regenerative capacity of cardiac tissue has long been an obstacle to treating damaged myocardium. Cell-based therapy offers an enormous potential to the current treatment paradigms. However, the efficacy of regenerative therapies remains limited by inefficient delivery and engraftment. Electrotaxis, electrically guided cell movement, has been clinically utilized to improve recovery in a number of tissues, but has not been investigated for treating myocardial damage.

Objectives—The goal of the study is to test the electrotactic behaviors of several types of cardiac cells.

Methods—Cardiac Progenitor Cells (CPCs), Cardiac Fibroblasts (CFs), and human induced Pluripotent Stem cell-derived Cardiac Progenitor Cells (hiPSC-CPCs) were used.

Results—CPCs and CFs electrotax towards the anode of a direct current electric field (EF), while hiPSC-CPCs electrotax toward the cathode. The voltage-dependent electrotaxis of CPCs and CFs requires the presence of serum in the media. Addition of soluble vascular cell adhesion molecule (sVCAM) to serum-free media restores directed migration. We provide evidence that CPC and CF electrotaxis is mediated through phosphatidylinositide 3-kinases (PI3′K) signaling. In addition, Very Late Antigen-4 (VLA4), an integrin and growth factor receptor, is required for electrotaxis and localizes to the anodal edge of CPCs in response to direct current EF. HiPSC-derived CPCs do not express VLA4, migrate toward the cathode in a voltage-dependent manner, and similar to CPCs and CFs require media serum and PI3′K activity for electrotaxis.

Corresponding Authors: Nipavan Chiamvimonvat and Padmini Sirish, Division of Cardiovascular Medicine, Department of Internal Medicine, University of California, Davis, One Shields Avenue, GBSF 6315, Davis, CA 95616; Department of Veterans Affairs, Northern California Health Care System, 10535 Hospital Way, Mather, CA 95655, voice: (530) 754-7158, fax: (530) 754-7167, nchiamvimonvat@ucdavis.edu and psirish@ucdavis.edu.

There is no conflict of interest

Conclusion—The electrotactic behaviors of these therapeutic cardiac cells may be utilized for improving cell-based therapy for recovering function in damaged myocardium.

Keywords

Electrotaxis; Cardiac progenitor cells; Cardiac fibroblasts; Human induced pluripotent stem cells; Soluble vascular cell adhesion molecule; Phosphatidylinositide 3-kinases

INTRODUCTION

Electrically guided migration, electrotaxis, is an important migratory mechanism involved in wound repair in multiple tissue types,[1–3] however, the role of electrotaxis in cardiac tissue remains largely unexplored. The migratory mechanisms of cardiac cells are especially relevant in cell-based therapies for recovery of cardiac function after injury. Indeed, wound electric fields are generated after myocardial infarction (MI) and have been recorded in large animal ST elevation MI as high as 38 V/cm.[4] Several cell types are currently being investigated for their potential roles in cardiac regeneration, including human induced pluripotent stem cells (hiPSCs) and adult cardiac progenitor cells (CPCs) which are positive for c-kit (Cluster of Differentiation CD117) and negative for lineage markers (c-kit+/Lin −)).[5] C-kit$^+$ cells have been the focus of extensive research.[5,6] While their role as significant source of cardiomyocytes remains controversial,[7,8] c-kit expressing cardiac cells' ability to differentiate down several cardiac specific lineages including endothelial cells,[7,9] smooth muscle cells,[10] and cardiac myocytes[10,11] makes them an important target for regenerative therapy.

Recent studies on electrotaxis have shown that receptor-ligand interactions are necessary for response to electric stimulation and extracellular chemical signaling is required for electrotaxis in multiple cell types. The salience of receptor-ligand interaction as an electrotaxis mechanism has been demonstrated using *in vitro* electrotaxis models of serum dependence,[12] ligand replacement,[13] and asymmetrical distribution of receptors during cell polarization.[14] Although electrotaxis in cardiac cells has not been described, CPCs express an integrin subunit, integrin β-1, that localizes to the leading edge of electrotaxing keratocytes.[15] The mouse homologue, integrin β-1, is a subunit of Very Late Antigen-4 (VLA4 or $\alpha_4\beta_1$ integrin) which has been shown to drive chemotactic migration in CPCs.[16]

Therefore, the goal of the current study is to test the responses of adult CPCs and hiPSC-derived CPCs (hiPSC-CPCs) to electric field (EF) and to determine the underlying mechanisms. Thymocyte antigen 1 (Thy 1.2 or CD90.2)-positive cardiac fibroblasts (CFs) are also used for comparison. Here we show that serum dependence of electrotaxis signaling is common to multiple cardiac cell types as well as that of hiPSC-CPCs. Additionally, the interactions between soluble vascular adhesion molecule (sVCAM) and VLA4 is necessary and sufficient for the activation of phosphatidylinositide 3-kinases (PI3′K)-mediated electrotaxis in CPCs and CFs. These insights may provide novel paradigms to enhance cell-based therapy for heart disease.

MATERIALS AND METHODS

Experiments were performed in compliance with a University of California, Davis Animal Care and Use Committee approved protocol and conform the NIH guidelines for the care and use of laboratory animals. Detailed Materials and Methods are provided in the Online Supplement.

Cell isolation and culture

Supplemental Figure 1 is a diagram depicting the isolation of CPCs (c-kit$^+$, lin$^-$) and CFs as well as differentiation of hiPSC-CPCs and selection for human c-kit expression.[11,17] A conditional knockout of *Integrin* α_4 gene (*ITGA4*) was induced as previously described[18] in age-matched, male, Mx.$cre^+\alpha 4^{flox/flox}$ C57BL/6 mice. Anesthesia for terminal surgery includes ketamine (50–80 mg/kg) and xylazine (5 mg/kg).

Experimental setup

Migration velocity and directedness scores were determined as previously described.[12] Velocity and total displacement of the cell was calculated and the angle of displacement relative to the EF plane was determined (θ). Directedness was calculated (cosine θ) and directedness towards the cathode receives a score of 1 and towards the anode receives a score of −1.

RESULTS

CPCs migrate towards the anode in a voltage-dependent manner

The electrotaxis of native, adult CPCs (c-kit$^+$, lin$^-$) was investigated using an *ex vivo*, unexpanded cell population to avoid unintended alterations in culture. Figure 1A–B is a diagram depicting a custom-designed electrotaxis chamber. Bright-field time-lapse microscopy was used to record the migration. The directedness of cell migration in the EF was voltage-dependent and directed towards the anode within the tested range (0–12 volts/cm (V/cm)) with the highest level at 10 and 12 V/cm. A negligible level of directedness towards the cathode was shown at 0 V/cm and significantly lower than that at the 8 V/cm condition ($p<0.01$) (Figure 1C). There was a linear relationship between directedness and EF strength of 0.052 degree of directedness·volt^{-1}·cm^{-1} ($R^2 = 0.97$). In contrast, the voltage-velocity relationship was nonlinear (Figure 1D). An example of the total displacement of individual cell migration is depicted by the scatter pattern in the circle diagram (Figure 1E) with circles delineating 500 μm and 1000 μm in a 300-minute 10 V/cm experiment. A bright-field image of CPCs under EF is depicted in Figure 1F.

CPC electrotaxis is serum- and sVCAM-dependent

We tested the hypothesis that CPC electrotaxis is regulated through sVCAM and VLA4 interaction along the PI3′K pathway (Figure 2A–D). Indeed, after 30 minutes of serum free conditions, CPCs did not migrate towards the anode at EF of 10 V/cm; directedness was reduced to levels not significantly different from 0 V/cm condition (Figure 2A). However, the migration velocity in serum free conditions increased significantly compared to control media ($p< 0.01$; Figure 2D).

Introducing 10 nM sVCAM to serum free media was sufficient to restore directedness to control levels. Moreover, inhibition of the receptor with anti-integrin α_4 (ITGA4, a VLA4 subunit) antibody lowered directedness to voltage-free levels but significantly increased the velocity of migration (Figure 2A, D). PI3′K is a downstream regulator of migratory directedness in multiple cell types.[16,19,20] Treatment with an inhibitor of PI3′K, wortmannin, resulted in a reduction of migratory directedness to negligible levels (Figure 2A, D).

We further used siRNA targeted against *ITGA4* to knockdown ITGA4 in CPCs. We confirmed the knockdown of *ITGA4 via* qPCR (Figure 2B). CPCs treated with *ITGA4* silencing siRNA showed a 24% reduction in migratory velocity and a significant reduction in migratory directedness (Figure 2A, D). In contrast, cells treated with non-silencing siRNA electrotaxed with normal directedness under 10 V/cm.

A conditional knockout of *ITGA4* mouse model (Mx.$cre^{+}\alpha 4^{flox/flox}$) was used. Electrotaxis of CPCs isolated from the knockout animals showed a significant reduction in electrotaxis towards the anode (Figure 2A). We further confirmed the significant knockdown in the expression of *ITGA4* in the mouse heart tissues using qPCR compared to ITGA4 expression in Mx.$cre^{+}\alpha 4^{flox/flox}$ mice without induction of Cre ($p< 0.01$, Figure 2C).

VLA4 localization towards the anode occurs in the absence of serum

VLA4 localization in CPCs was tested under control (Figure 2E) and EF stimulation (10 V/cm) for 3 hours (Figure 2F). EF stimulation yielded side-specific orientation of VLA4 towards the leading edge at the anodal side of CPCs (Figure 2F) compared to the random localization of VLA4 in control (0 V/cm) (Figure 2E). In the absence of serum, CPCs exposed to EF stimulation (10 V/cm) for 3 hours showed side-specific localization of VLA4 towards the anode (Figure 2G–H) similar to that of CPCs in serum rich media. Analysis of the asymmetrical distribution of VLA4 in 10 V/cm EF showed anodal localization with asymmetrical index (AI) of 0.145 ± 0.051 and 0.246 ± 0.077 for serum free and serum conditions, respectively, compared to −0.015±0.044 in the 0 V/cm condition (Figure 2I, see Detailed Online Materials and Methods). CPCs also maintained expression of c-kit in the absence and presence of EF stimulation, with or without serum in the growth media.

CFs migrate toward the anode in a voltage-dependent manner

Using a similar *ex vivo* model, CFs also electrotaxed towards the anode in a voltage-dependent manner using the tested range of 0–8 V/cm with the highest level of directedness at 8 V/cm (Figure 3A and Supplemental Video 1). EF strength of 10 V/cm was tested but resulted in cell damage and death and was not used further. A negligible level of directedness towards the anode was observed at 0 V/cm (Supplemental Video 2). The voltage-directedness relationship in CFs is roughly linear with a 0.13 unit of directedness·volt^{-1}·cm^{-1} (R^2= 0.86, Figure 3A). However, the relationship between voltage and velocity was nonlinear (Figure 3B). The total cell displacement from the initial cell coordinates is depicted in Figure 3C. CFs are larger than CPCs or hiPS-CPCs and have more cytoplasm per cell (Figure 3D). As an internal control, EF orientation was reversed after 2

hours of electrotaxis showing that CF directedness was towards the anode both before and after the reorientation of the EF (Supplemental Figure 2).

CF Electrotaxis is serum- and sVCAM-dependent

The serum dependence of CF electrotaxis was demonstrated with a total loss of migratory directedness in the absence of serum (Figure 3E). However, the migration velocity in serum free conditions increased significantly (Figure 3F). Application of 10 nM sVCAM to serum free media restored directedness to control media levels. PI3′K inhibition with wortmannin abolished the migratory directedness of CFs. Contrasting to the loss of adhesion seen in CPCs after wortmannin exposure, CFs maintained adherence to the matrigel substrate.

The application of anti-ITGA4 antibody to CFs showed a reversal of migratory directedness to 0.15 ± 0.056 towards the cathode. This reversed directedness was significantly different from 0 V/cm EF stimulation ($p < 0.001$) and had a directedness that was between and statistically different from 4 and 6 V/cm field strengths (Figure 3A and E). CFs isolated from Mx.$cre^{+}\alpha4^{flox/flox}$ mice showed a significant loss of migratory directedness with a score which is not significantly different from the 0 V/cm (Figure 3E). Similar to CPCs, CFs also responded to the knockdown of ITGA4 and wortmannin treatment with significant increases in velocity of migration (Figure 3F).

hiPS-CPCs Migrate Towards the Cathode in a Voltage-Dependent manner

In contrast to CPCs and CFs, the electrotaxis response of hiPSC-CPCs was directed toward the cathode in a voltage-dependent manner within the tested range (0–8 V/cm, Figure 4A). Voltage-directedness relationship was best described by an exponential function: $y = 0.0039e^{x/1.63821}$ ($R^2 = 0.99$). The voltage-velocity relationship in hiPSC-CPCs is nonlinear (Figure 4B). The complex behavior of individual cell migration is depicted by the scatter pattern shown in the circle diagram (Figure 4C) while a bright-field image of hiPSC-CPCs in culture is depicted in Figure 4D.

HiPSC-CPC electrotaxis is serum dependent

The serum dependence of hiPSC-CPC electrotaxis was supported by the reduced directedness of migration in the absence of serum ($p<0.05$, Figure 4E). PI3′K was also necessary for directed migration as the addition of the inhibitor, wortmannin, significantly reduced directedness (Figure 4E). Similar to CPCs, hiPSC-CPCs also responded to the absence of serum and wortmannin treatment with significant increases in velocity of migration (Figure 4F). However, unlike CPCs and CFs, hiPS-CPCs do not express VLA4. This was confirmed using immunofluorescence confocal imaging using anti-ITGA4 antibodies and qPCR. Human coronary endothelial cells (hEC) and hiPSCs were used as positive and negative controls, respectively[21] (Figure 4G–H). We also tested the differentiation ability of hiPSC-CPCs into cardiomyocytes by quantifying the expression of myosin heavy chain (MHC) using differentiation protocol as described in one recent study in induced-CPCs (iCPCs) where ~13% of iCPCs are c-kit^{+}.[22] Supplementary Figure 3A shows 6.5 ± 0.3% MHC positivity after 20 days of differentiation.

The lamellipodia CPCs, CFs, and hiPSC-CPCs are organized towards the leading edges of electrotaxing cells with CPCs and CFs localizing to the anodal end while hiPSC-CPCs localize towards the anode (Supplemental Figure 3B–D). Finally, to directly rule out that the EF may cause the redistribution of sVCAM, we performed western blots analyses to quantify the levels of sVCAM on anodal and cathodal sides in the matrigel. There are no differences in the localization of the sVCAM after EF stimulation (Supplemental Figure 4 A–C).

DISCUSSION

The role of electrotaxis as a migratory stimulus in the heart has been proposed[23] but has not been unexplored. Understanding the effects of EF and guidance mechanisms in electrically active tissue is imperative for directing the localization of both endogenous and exogenous cell-based therapy. In the current study, we demonstrate that these cells migrate in EF in a voltage- and serum-dependent manner with CPCs and CFs electrotaxing *via* sVCAM/VLA4 signaling. Moreover, our results support the mechanistic model of receptor orientation in eletrotaxis (Figure 5).

Critical roles of VLA4-sVCAM and PI3′K signaling in CPC electrotaxis

CPCs migrate towards the anode under direct current EF stimulation in a voltage- and serum-dependent manner *via* VLA4-sVCAM signaling through PI3′K. Serum dependence for electrotaxis has been described in corneal epithelial cells[12] and keratinocytes[24] indicating that extracellular chemical mediators are often required for electrotaxis. The removal of media serum reduced the migratory directedness of CPCs indicating that one or multiple serum components are necessary for migration. However, the absence of serum did not affect the asymmetrical distribution of the receptor VLA4 to the leading edge of CPCs (Figure 2E–F). The data suggest that the polarization of integrins on the membrane is independent of, and could precede migratory directedness and be involved in the sensing of the EF. Electrically stimulated asymmetrical distribution of integrins has been previously reported in other cell types[14] but this is the first instance of such a distribution in the absence of migratory directedness (Figure 2A, E–I).

VLA4 is a known chemoattractant for CPCs[16] and interacts with sVCAM, a soluble component of fetal bovine serum. While the absence of serum in the media abolished directedness, adding sVCAM to serum free media was sufficient to restore the migratory directedness to control levels (Figure 2A). Although this finding does not exclude the possible contribution of other chemical drivers of electrotaxis, it demonstrates the salient importance of sVCAM and its receptor VLA4 to electrotaxis. The critical roles of PI3′K were demonstrated in our study using wortmannin, which abolished migratory directedness.

Mechanistic underpinnings for CF electrotaxis

CFs play multiple roles in cardiac recovery, both providing physiological regulatory functions and pathological cardiac remodeling.[25,26] Thy 1.2^{+} CFs have a strong directedness response and electrotax towards the anode in a voltage-dependent manner. The mechanism of CF electrotaxis operates along the same sVCAM-VLA4 ligand-receptor pathway as CPCs

with a few notable differences. The serum dependence of migration and sufficiency of sVCAM to restore the loss of function to control levels is similar to that of CPCs and the effect of PI3′K inhibition with wortmannin is also similar. However, the inhibition of VLA4 function with anti-ITGA4 antibody reversed the direction of migration to a significant cathodal orientation. The presence of serum provides a number of ligands that could be responsible for the reversed electrotaxis which, in the absence of VLA4 activity, activates a normally secondary or even suppressed pathway to direct migration towards the cathode. Mechanisms dependent on cAMP and cGMP have been shown to direct migration in cell fragments in the opposite direction of the intact cell[20,27] indicating that opposing electrotactic drivers within a cell may be the norm rather than an exception. The use of Mx.$cre^{+}\alpha 4^{flox/flox}$ mice as a source of *ITGA4* KO CFs shows that the loss of ITGA4 inhibits the anodal orientation of CF electrotaxis (Figure 3E).

HiPSC-CPCs electrotax towards the cathode

HiPSCs have been the focus of an ever increasing number of experimental applications as a model for disease, a potential source of therapeutic cells,[28] and an attractive platform for drug screening. The availability and flexibility without the ethical predicament of embryonic stem cells makes it a compelling cell type and when derived into c-kit^{+}/lin^{-} cardiac progenitor cells (hiPSC-CPC), may be applied to regenerative therapy. Interestingly, hiPSC-CPCs also respond to EF stimulation in a voltage-dependent manner but do so in the opposite field orientation to that of CPCs, toward the cathode. In addition, the directionality is the opposite of the electrotactic response of undifferentiated hiPSCs,[29] however, the exact mechanisms underlying this difference along the differentiation process remain to be investigated. Similar to CPCs, hiPS-CPC electrotaxis was also shown to be serum-dependent and regulated by PI3′K (Figure 4E). However, hiPS-CPCs do no express VLA4 (Figure 4G–H) and the specific factors required for electrotaxis remain to be identified. Indeed, the cathodal migration of hiPS-CPCs may be utilized for *in vivo* cardiac injury models because the center of tissue damage has been reported to generate a local cathode.[19]

Summary and future directions

In summary, the current study demonstrates for the first time the electrotaxis behaviors of adult CPCs and CFs as well as that of hiPS-CPCs and provides mechanistic insights into the ligand-receptor dependence of EF-guided directedness in these cells. The VLA4 orientation in response to the EF takes place independently of the presence of the ligand but the ligand is required for the activation of migratory directedness. This suggests that the cells may sense the EF through mechanisms which are independent of soluble factors in the media but additional studies are required to determine the precise mechanism of EF detection. Clearly more research needs to be performed to identify the electrotactic response of specific cardiac cell populations in order to bring the potential benefits of EF therapy to cardiac tissue.

Supplementary Material

Refer to Web version on PubMed Central for supplementary material.

Acknowledgments

We would like to thank Dr. Thalia Papayannopoulou (University of Washington) for Mx.$cre^{+}\alpha 4^{flox/flox}$ mice.

FUNDING SOURCES

This work was supported by NIH R01 HL085727, NIH R01 HL085844, NIH R01 HL137228, the Rosenfeld Foundation award, VA Merit Review Grant I01 BX000576 and I01 CX001490 to NC, Postdoctoral Fellowship award to BJF from NIEHS Superfund to BD Hammock, Postdoctoral Fellowship awards to PS from NIH T32 Training Grant in Basic and Translational Medicine (NIH HL08350), California Institute for Regenerative Medicine, Stem Cell Training Program (TG2-01163) and American Heart Association Postdoctoral Fellowship Award. NC is the holder of the Roger Tatarian Endowed Professorship in Cardiovascular Medicine.

References

1. Schatz A, Rock T, Naycheva L, Willmann G, Wilhelm B, Peters T, Bartz-Schmidt KU, Zrenner E, Messias A, Gekeler F. Transcorneal electrical stimulation for patients with retinitis pigmentosa: a prospective, randomized, sham-controlled exploratory study. Invest Ophthalmol Vis Sci. 2011; 52:4485–4496. [PubMed: 21467183]
2. Polak A, Franek A, Taradaj J. High-Voltage Pulsed Current Electrical Stimulation in Wound Treatment. Advances Wound Care. 2014; 3:104–117.
3. Shi HF, Xiong J, Chen YX, Wang JF, Qiu XS, Wang YH, Qiu Y. Early application of pulsed electromagnetic field in the treatment of postoperative delayed union of long-bone fractures: a prospective randomized controlled study. BMC Musculoskelet Disord. 2013; 14:35. [PubMed: 23331333]
4. Kleber AG, Janse MJ, Van Capelle FJ, Durrer D. Mechanism and time course of ST and TQ segment changes during acute regional myocardial ischemia in the pig heart determined by extracellular and intracellular recordings. Circ Res. 1978; 42:603–613. [PubMed: 639183]
5. Broughton KM, Sussman MA. Empowering Adult Stem Cells for Myocardial Regeneration V2.0: Success in Small Steps. Circ Res. 2016; 118:867–880. [PubMed: 26941423]
6. Beltrami AP, Barlucchi L, Torella D, et al. Adult cardiac stem cells are multipotent and support myocardial regeneration. Cell. 2003; 114:763–776. [PubMed: 14505575]
7. Sultana N, Zhang L, Yan J, Chen J, Cai W, Razzaque S, Jeong D, Sheng W, Bu L, Xu M. Resident c-kit^{+} cells in the heart are not cardiac stem cells. Nature Communications. 2015; 6
8. Van Berlo JH, Kanisicak O, Maillet M, Vagnozzi RJ, Karch J, Lin S-CJ, Middleton RC, Marbán E, Molkentin JD. C-kit^{+} cells minimally contribute cardiomyocytes to the heart. Nature. 2014; 509:337. [PubMed: 24805242]
9. Vajravelu BN, Hong KU, Al-Maqtari T, Cao P, Keith MC, Wysoczynski M, Zhao J, Moore JB IV, Bolli R. C-Kit promotes growth and migration of human cardiac progenitor cells via the PI3K-AKT and MEK-ERK pathways. PloS One. 2015; 10:e0140798. [PubMed: 26474484]
10. Messina E, De Angelis L, Frati G, Morrone S, Chimenti S, Fiordaliso F, Salio M, Battaglia M, Latronico MV, Coletta M. Isolation and expansion of adult cardiac stem cells from human and murine heart. Circ Res. 2004; 95:911–921. [PubMed: 15472116]
11. Sirish P, Lopez JE, Li N, Wong A, Timofeyev V, Young JN, Majdi M, Li RA, Chen HS, Chiamvimonvat N. MicroRNA profiling predicts a variance in the proliferative potential of cardiac progenitor cells derived from neonatal and adult murine hearts. J Mol Cell Cardiol. 2012; 52:264–272. [PubMed: 22062954]
12. Zhao M, Agius-Fernandez A, Forrester JV, McCaig CD. Orientation and directed migration of cultured corneal epithelial cells in small electric fields are serum dependent. J Cell Sci. 1996; 109:1405–1414. [PubMed: 8799828]
13. Meng X, Arocena M, Penninger J, Gage FH, Zhao M, Song B. PI3K mediated electrotaxis of embryonic and adult neural progenitor cells in the presence of growth factors. Exp Neurol. 2011; 227:210–217. [PubMed: 21092738]
14. Huang L, Cormie P, Messerli MA, Robinson KR. The involvement of Ca^{2+} and integrins in directional responses of zebrafish keratocytes to electric fields. J Cell Physiol. 2009; 219:162–172. [PubMed: 19097066]

15. Han J, Yan X-L, Han Q-H, Li Y-J, Du Z-J, Hui Y-N. Integrin β1 subunit signaling is involved in the directed migration of human retinal pigment epithelial cells following electric field stimulation. Ophthalmic Res. 2010; 45:15–22. [PubMed: 20720436]
16. Matsuura K, Honda A, Nagai T, Fukushima N, Iwanaga K, Tokunaga M, Shimizu T, Okano T, Kasanuki H, Hagiwara N, Komuro I. Transplantation of cardiac progenitor cells ameliorates cardiac dysfunction after myocardial infarction in mice. J Clin Invest. 2009; 119:2204–2217. [PubMed: 19620770]
17. Sirish P, Li N, Liu J-Y, Lee KSS, Hwang SH, Qiu H, Zhao C, Ma SM, López JE, Hammock BD, Chiamvimonvat N. Unique mechanistic insights into the beneficial effects of soluble epoxide hydrolase inhibitors in the prevention of cardiac fibrosis. Proc Natl Acad Sci USA. 2013; 110:5618–5623. [PubMed: 23493561]
18. Scott LM, Priestley GV, Papayannopoulou T. Deletion of α4 integrins from adult hematopoietic cells reveals roles in homeostasis, regeneration, and homing. Mol Cell Biol. 2003; 23:9349–9360. [PubMed: 14645544]
19. Zhao M, Song B, Pu J, Wada T, Reid B, Tai G, Wang F, Guo A, Walczysko P, Gu Y. Electrical signals control wound healing through phosphatidylinositol-3-OH kinase-γ and PTEN. Nature. 2006; 442:457–460. [PubMed: 16871217]
20. Sun Y, Do H, Gao J, Zhao R, Zhao M, Mogilner A. Keratocyte fragments and cells utilize competing pathways to move in opposite directions in an electric field. Current Biol. 2013; 23:569–574.
21. Rowland TJ, Miller LM, Blaschke AJ, Doss EL, Bonham AJ, Hikita ST, Johnson LV, Clegg DO. Roles of integrins in human induced pluripotent stem cell growth on Matrigel and vitronectin. Stem Cells Dev. 2010; 19:1231–1240. [PubMed: 19811096]
22. Lalit PA, Salick MR, Nelson DO, et al. Lineage Reprogramming of Fibroblasts into Proliferative Induced Cardiac Progenitor Cells by Defined Factors. Cell Stem Cell. 2016; 18:354–367. [PubMed: 26877223]
23. Lujan HL, DiCarlo SE. Mimicking the endogenous current of injury improves post-infarct cardiac remodeling. Med Hypotheses. 2013; 81:521–523. [PubMed: 23871584]
24. Fang KS, Farboud B, Nuccitelli R, Isseroff RR. Migration of human keratinocytes in electric fields requires growth factors and extracellular calcium. J Invest Dermatol. 1998; 111:751–756. [PubMed: 9804333]
25. Baudino TA, Carver W, Giles W, Borg TK. Cardiac fibroblasts: friend or foe? Am J Physiol Heart Circ Physiol. 2006; 291:H1015–1026. [PubMed: 16617141]
26. Souders CA, Bowers SL, Baudino TA. Cardiac fibroblast the renaissance cell. Circ Res. 2009; 105:1164–1176. [PubMed: 19959782]
27. Zhu K, Sun Y, Miu A, Yen M, Liu B, Zeng Q, Mogilner A, Zhao M. cAMP and cGMP Play an Essential Role in Galvanotaxis of Cell Fragments. J Cell Physiol. 2016; 6:1291–1300.
28. Jung Y, Bauer G, Nolta JA. Concise Review: Induced Pluripotent Stem Cell-Derived Mesenchymal Stem Cells: Progress Toward Safe Clinical Products. Stem Cells. 2012; 30:42–47. [PubMed: 21898694]
29. Zhang J, Calafiore M, Zeng Q, Zhang X, Huang Y, Li RA, Deng W, Zhao M. Electrically guiding migration of human induced pluripotent stem cells. Stem Cell Rev. 2011; 7:987–996. [PubMed: 21373881]

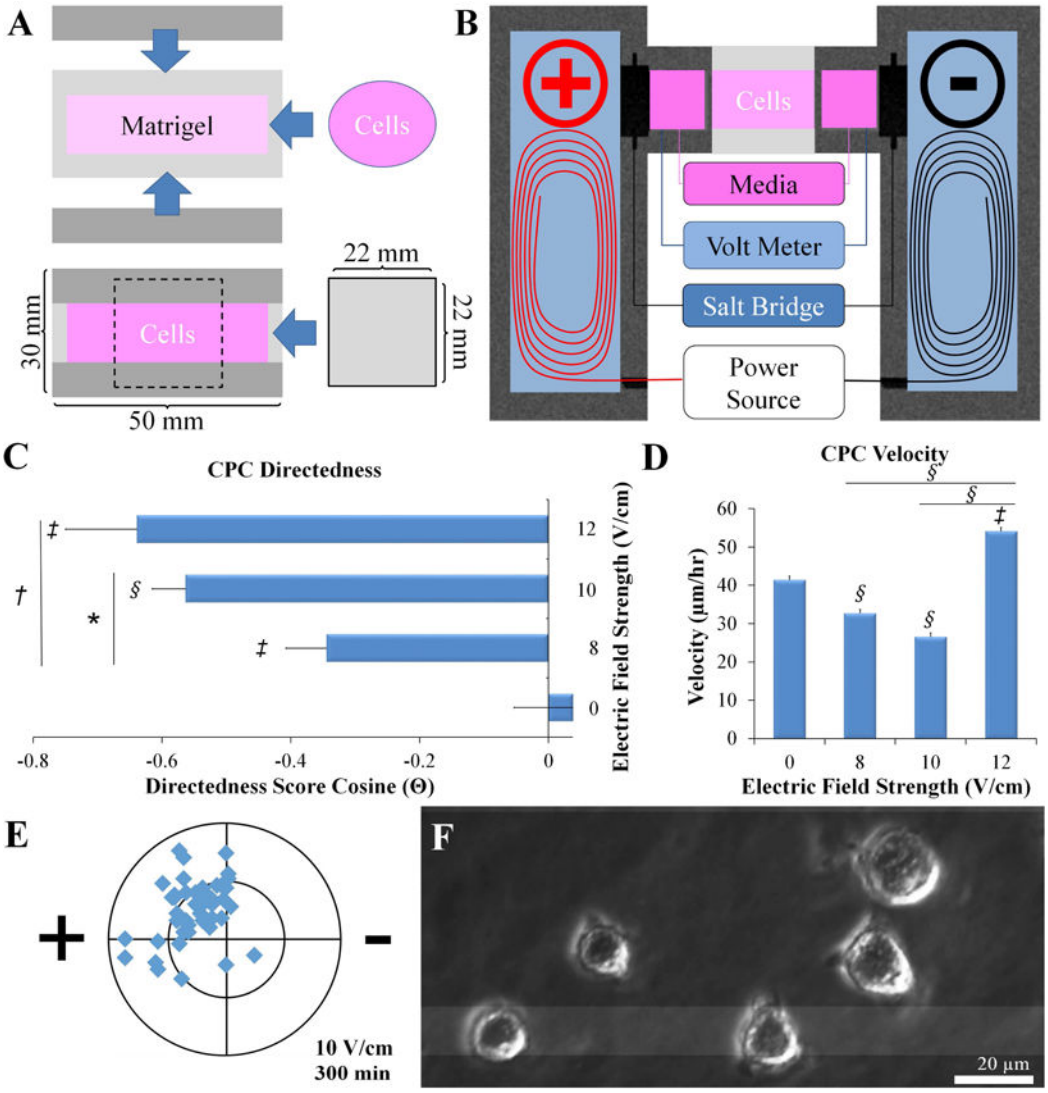

Figure 1. Migration chamber for *in vitro* electrotaxis

A) A 30.8 mm^3 glass chamber is constructed using covers slips. B) Glass chamber is attached to a custom-designed electrotaxis apparatus and stimulated with a constant voltage DC power source. C) Constant EF stimulation of CPCs increased migratory directedness in a voltage-dependent manner towards the anode. D) Voltage *vs.* velocity shows nonlinear but significant relationship to field strength. E) Cell translocation from the origin is plotted in a circle diagram for CPCs at 10 V/cm for 300 min, inner and outer circles are 500 and 1000 μm, respectively. F) Bright field image of CPCs during migration. (n=49, 81, 62, and 18 cells for EF strengths of 0, 8, 10 and 12 V/cm, respectively; *p<0.05, †p<0.01, ‡p<0.001, and §p<0.0001).

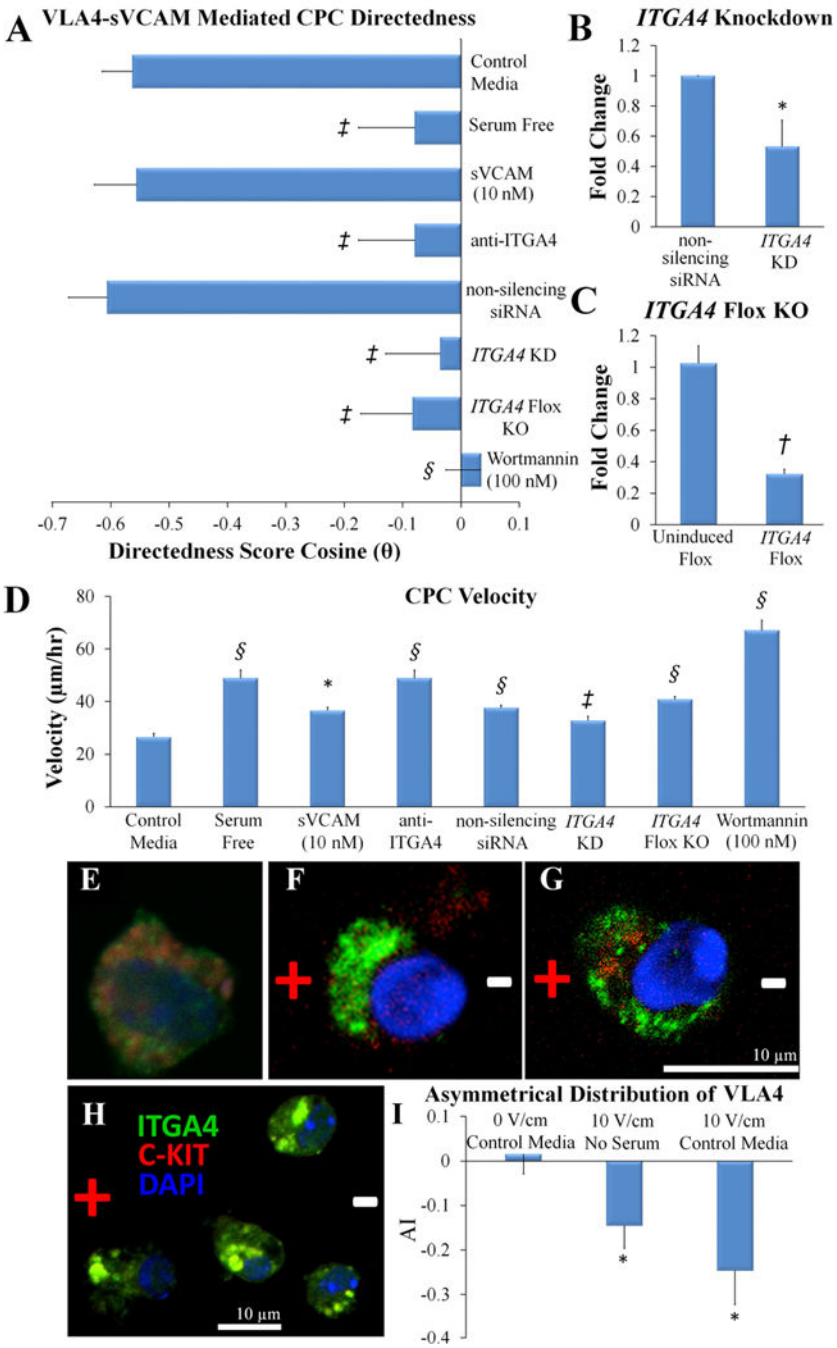

Figure 2. CPC electrotaxis is regulated *via* sVCAM-VLA4-PI3′K interaction

A) Directedness of CPC migration was significantly reduced using anti-ITGA4 antibody, siRNA against *ITGA4* (*ITGA4* KD), conditional knockout of *ITGA4* (*ITGA4* Flox KO), wortmannin, and serum free conditions. In contrast, directedness of CPC migration at 10 V/cm was not affected by non-silencing siRNA, and was restored by sVCAM (n=62, 60, 62, 58, 145, 81, 68, and 66 cells for control media with serum, serum free media, serum free media with 10 nM sVCAM, after exposure to anti-ITGA4 antibody, after exposure to wortmannin, CPCs treated with non-silencing siRNA, CPCs treated with *ITGA4* silencing

siRNA, and *ITGA4* conditional KO, respectively). B, C) qPCR analyses demonstrating the reduction of *ITGA4* mRNA after knockdown using siRNA and after induction of *Cre recombinase* shown as fold change (n=4–5 samples). D) Velocity of CPCs was significantly increased from control conditions in all treated groups with the highest velocity in the wortmannin treated group. E–H) Immunofluorescence confocal microscopic imaging showing VLA4 subunit, ITGA4, labeled with FITC (green), c-kit stained with Alexa 555 (red) and DAPI nuclear counterstain (blue). E) Diffuse ITGA4 staining pattern in untreated CPC. F & G) ITGA4 localization to the anode in CPC after 3 hr treatment with 10 V/cm in media with and without serum, respectively. H) Effects of EF treatment without serum at lower magnification. I) Asymmetry index (AI) of VLA4 shows significant anodal distribution in 10 V/cm treatment in media without and with serum compared to 0 V/cm treatment (n=20 for each group) (*$p<0.05$, †$p<0.01$, ‡$p<0.001$, and §$p<0.0001$).

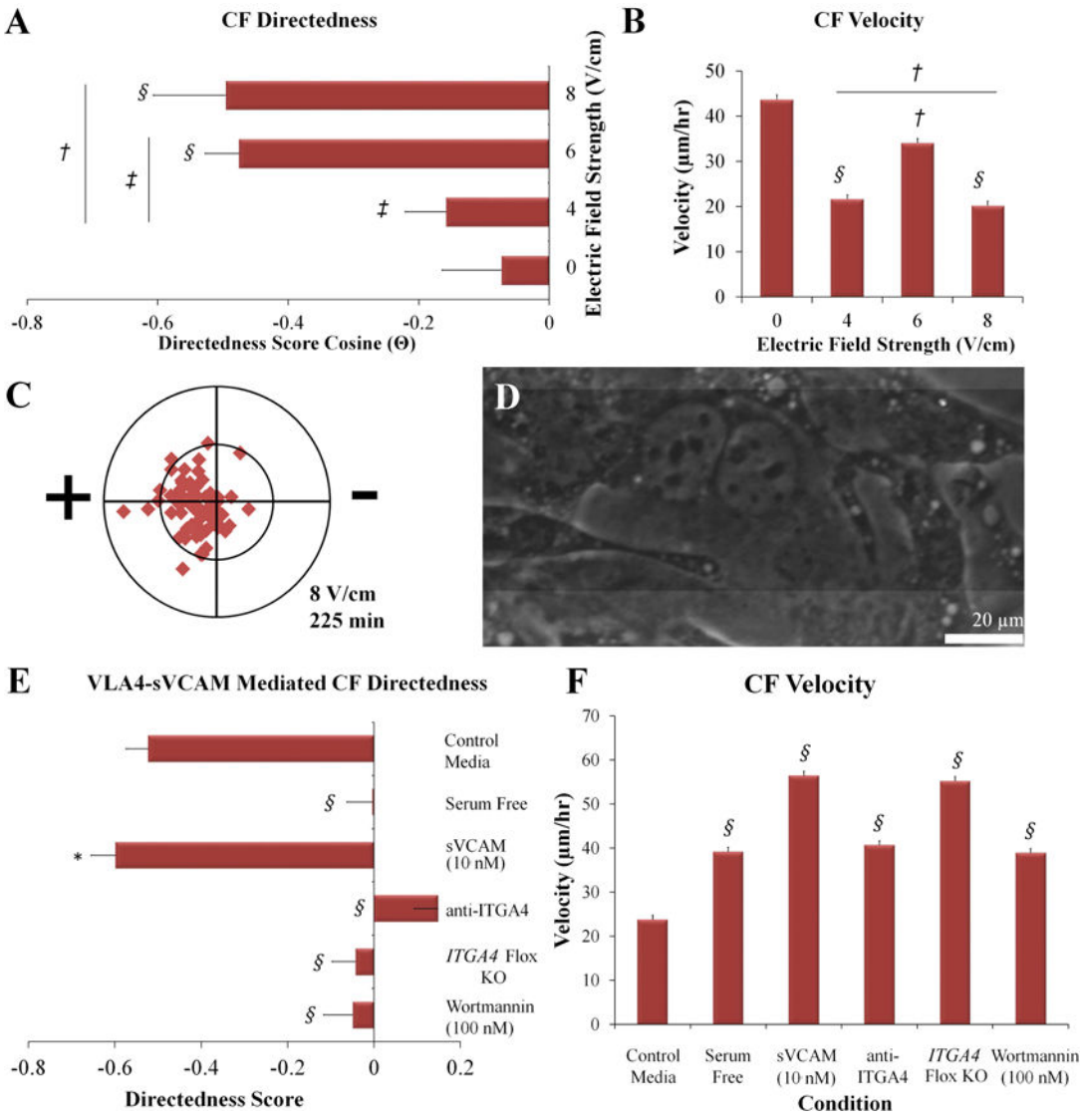

Figure 3. CF electrotaxis regulated *via* voltage and sVCAM-VLA4-PI3′K interaction

A) Constant EF stimulation of CFs increased migratory directedness in a voltage-dependent manner towards the anode. B) Voltage *vs.* velocity show nonlinear but significant relationship to field strength. C) Cell translocation from the origin is plotted in a circle diagram under EF of 8 V/cm for 225 min. (inner and outer circles are 100 and 200 μm, respectively). D) Bright field image of CFs during migration. (n=45, 57, 132 and 86 cells for 0, 4, 6, and 8 V/cm, respectively). E) Directedness of CF migration under 8 V/cm of constant EF stimulation was significantly reduced from control conditions in anti-ITGA4 antibody, wortmannin, and serum free conditions and was restored by sVCAM. F) Velocity of CFs was significantly increased from control conditions under all other conditions (n=72, 138, 50, 164, and 129 cells for control media with serum, serum free media, serum free media with 10 nM sVCAM, after exposure to anti-ITGA4 antibody, and after exposure to wortmannin, respectively. *p<0.05, †p<0.01, ‡p<0.001, and §p<0.0001).

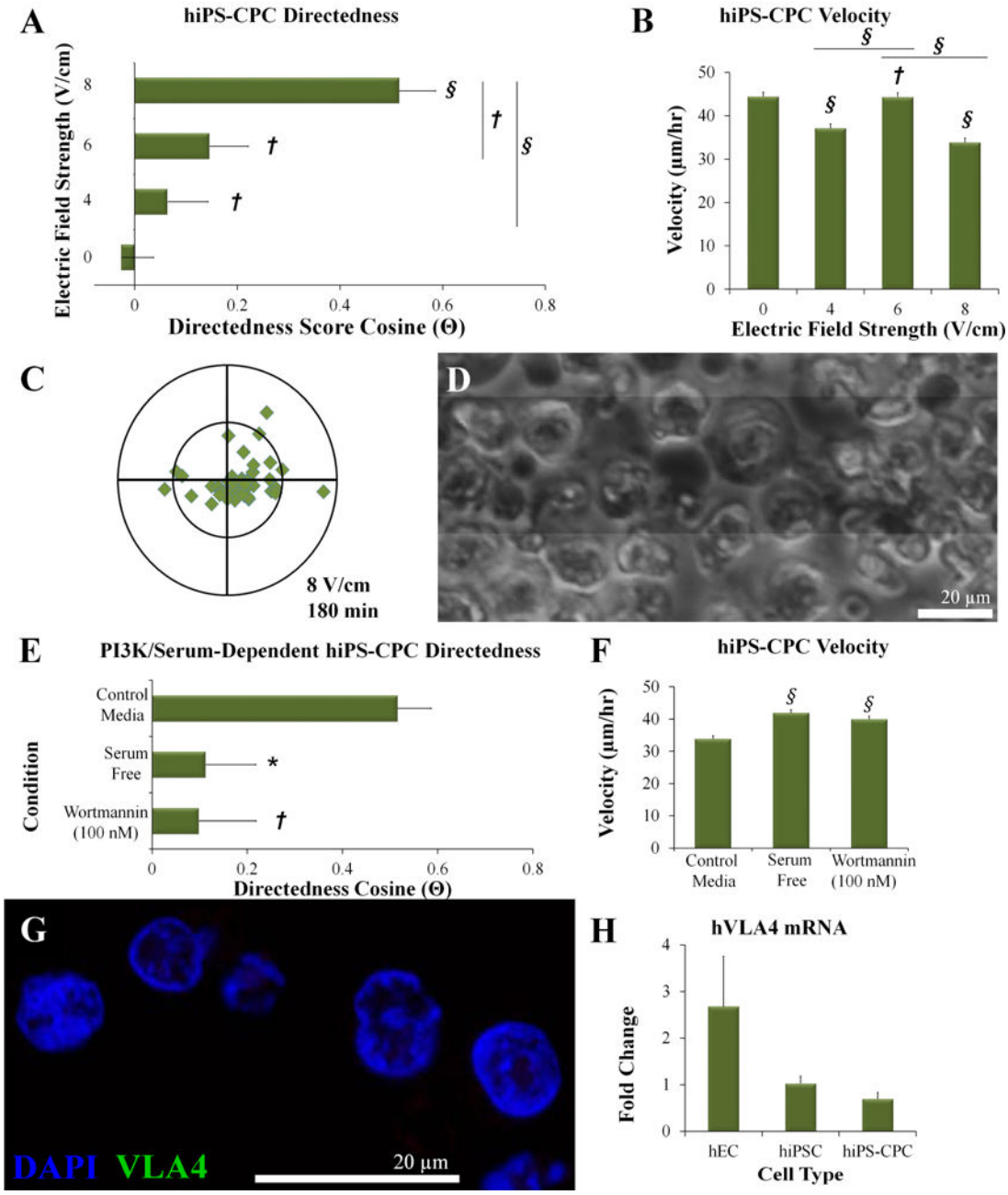

Figure 4. hiPS-CPC electrotaxis is regulated *via* voltage and serum-PI3′K interaction

A) Constant EF stimulation of hiPS-CPCs increased migratory directedness in a voltage-dependent manner towards the cathode. B) Voltage *vs.* velocity shows nonlinear but significant relationship to field strength (n=117, 71, 106, and 76 cells for 0, 4, 6, and 8 V/cm, respectively for Panels A–B). C) Cell translocation from the origin is plotted in a circle diagram under 8 V/cm constant EF stimulation for 180min (inner and outer circles are 75 and 150 μm, respectively). D) Bright field image of hiPS-CPCs during migration experiments. E) Directedness of hiPS-CPC migration under 8 V/cm EF stimulation was significantly reduced from control conditions in both wortmannin and serum free conditions. F) Velocity of hiPS-CPCs was significantly increased from control conditions in serum free

media and after application of wortmannin (n=76, 58, and 40 for control media with serum, serum free media, and after exposure to wortmannin, respectively). G) Absence of VLA4 subunit, ITGA4, labeled with FITC (green) and DAPI nuclear counterstain (blue) in hiPS-CPCs. H) Absence of *ITGA4* in hiPS-CPCs confirmed through qPCR analyses. Fold change for transcript expression of *ITGA4* for coronary endothelial cell (hEC), hiPSC, and hiPS-CPC normalized to *ITGA4* expression in hiPSC. The housekeeping gene, GAPDH, was used to control for loading (*$p<0.05$, †$p<0.01$, ‡$p<0.001$, and §$p<0.0001$).

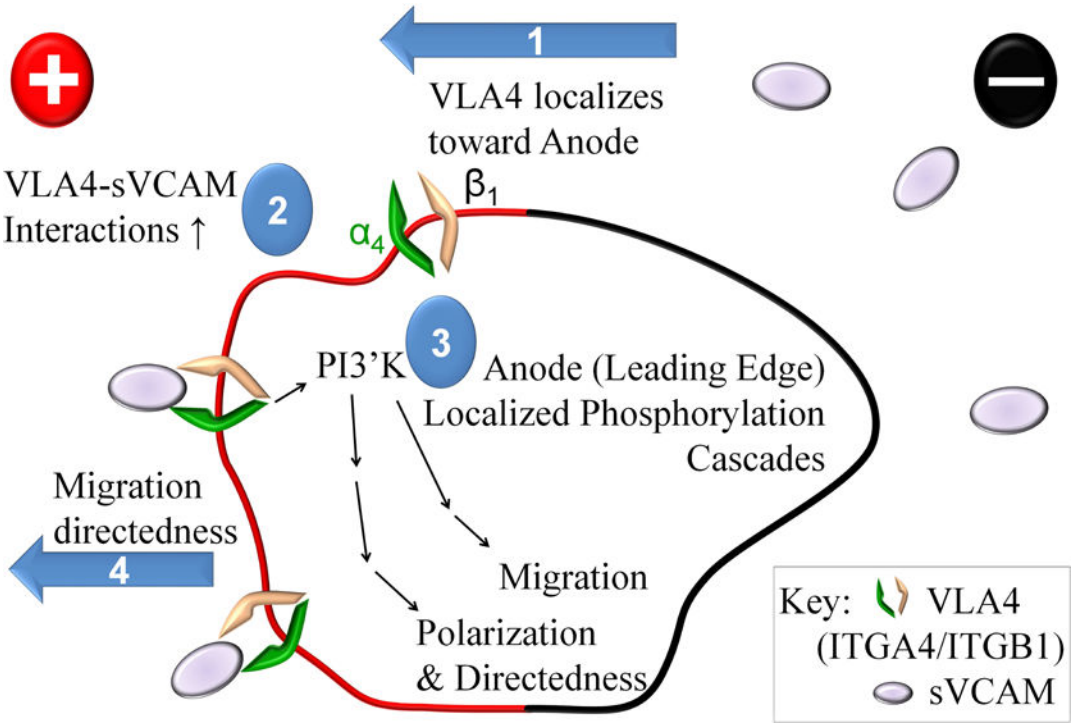

Figure 5. Summary of proposed mechanisms for CPC electrotaxis

Phase 1: VLA4 localization in the EF. Phase 2: Increased VLA4-sVCAM interactions on the leading edge, Phase 3: PI3′K phosphorylation activity, Phase 4: Migration towards the Anode in the constant EF.